

Dependence of CCT and CRI on the variable excitation wavelength and on the weight ratio of the phosphor in polydimethylsiloxane

JAN JARGUS^a, JAN NEDOMA^{a,*}, RADEK MARTINEK^b

^a*Department of Telecommunications, Faculty of Electrical Engineering and Computer Science, VSB - Technical University of Ostrava, 17. listopadu 15/2172, 708 33 Ostrava, Czech Republic*

^b*Department of Cybernetics and Biomedical Engineering, Faculty of Electrical Engineering and Computer Science, VSB - Technical University of Ostrava, 17. listopadu 15/2172, 708 33 Ostrava, Czech Republic*

This paper examines how the variable excitation wavelength affects CCT (correlated colour temperature) and CRI (colour rendering index) of the light generated by the luminescent layer. Two types of samples with a defined layer thickness and with a defined weight ratio of the YAG:Ce (cerium-doped yttrium aluminium) phosphor in PDMS (polydimethylsiloxane) were used. The measurements were performed in the wavelength range from 440 nm to 470 nm. The measurement results indicate that by using a suitable excitation wavelength and a suitable phosphor weight ratio in a luminescent layer of a defined thickness, the CCT and CRI parameters can be optimized.

(Received August 7, 2018; accepted June 14, 2019)

Keywords: CRI, CCT, PDMS, Spectral characteristic, YAG:Ce phosphor

1. Introduction

For the production of white light, the YAG:Ce phosphor in conjunction with a blue LED (light emitting diode) chip has been used for a long period of time. The quality of the white light created is primarily described by the CRI and CCT parameters. This topic is the content of many publications that mainly relate to white LEDs (white LED-WLED).

For example, [1-6] describes a method of producing the different WLEDs.

The YAG:Ce phosphor can be contained in various host substances and thus luminescent layers with different properties are formed. Glass and ceramics are often used as a host substance. The publications [7-10] deal with this theme. For instance, the article [10] introduces the production of transparent $\text{Ce:Y}_3\text{Al}_5\text{O}_{12}$ glass ceramics using spontaneous crystallization of $\text{PbO-SiO}_2\text{-Al}_2\text{O}_3\text{-Y}_2\text{O}_3\text{-B}_2\text{O}_3\text{Ce}^{3+}$ glass during the melting process. This LED emitting white light based on glass ceramic materials reached a correlated colour temperature of 5.561 K and a colour rendering index of 69.3.

The luminescent layer of the YAG:Ce phosphor and PDMS mixture has been used primarily for lighting because PDMS is also known as a host substance. For example, articles [11-15] address this topic and a thin luminescent film made from PDMS, which exhibited good thermal stability in the range from -50 to 230 °C, was presented in the article [15]. Furthermore, white LEDs were produced using a prepared YAG-doped luminescent

film having an average CCT value of 6.925 K, a CRI value of 71 and a mean luminous intensity of 115.7 lm/W.

The articles [16-17] also deal with the issue of the YAG:Ce phosphor located in the PDMS and the influence of the thickness of the luminescent layer on the resulting CCT of the white light generated by this layer is examined.

The above-mentioned publications do not deal with the combined influence of the variable excitation wavelength and the defined weight ratio of the YAG:Ce phosphor in the luminescent layer on the parameters describing the quality of white light. Our motivation was to examine in more detail the influence of the input parameters, i.e. the variable excitation wavelength and the defined luminescent layer parameters, on the resulting CCT and CRI values. The contribution of the article is the analysis of the suitable input parameters in order to optimize the procedures for obtaining white light with the desired qualitative parameters.

2. Methods

Phosphors are substances that can partially absorb excitation energy and then emit it with a spectrum different from the excitation spectrum. Absorption of the narrow blue excitation light, which is converted by the phosphor to a range of approximately 500 to 700 nm, is one of the possibilities of white light production. Since a portion of the blue excitation light remains unchanged by the phosphor, the combination of this residual blue light

with the converted broadband light is perceived by the human eye as white light.

2.1. CIE 1931 chromaticity coordinates and CCT

A light source with the emission spectrum $P(\lambda)$ produces tristimulus values X , Y and Z that characterize the colour perception of this light source $P(\lambda)$ in the eye. The equations for calculating the tristimulus values X , Y and Z are given below:

$$X = \int_{\lambda} \bar{x}(\lambda)P(\lambda) d\lambda \quad (1)$$

$$Y = \int_{\lambda} \bar{y}(\lambda)P(\lambda) d\lambda \quad (2)$$

$$Z = \int_{\lambda} \bar{z}(\lambda)P(\lambda) d\lambda \quad (3)$$

The colour-matching functions $\bar{x}(\lambda)$, $\bar{y}(\lambda)$ and $\bar{z}(\lambda)$ were set in 1931 by the International Commission on Illumination (Commission Internationale de l'Éclairage-CIE) and refer to the corresponding eye receptors sensitive to red, green and blue colours [18]. The graphs of these functions are shown in Fig. 1.

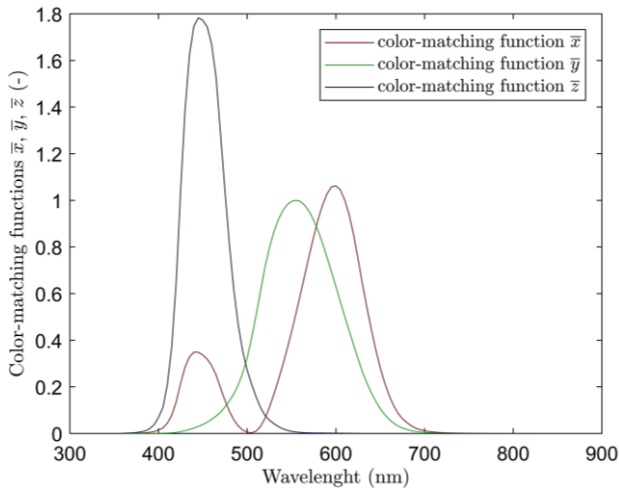


Fig. 1. Colour-matching functions (CIE 1931)

From the tristimulus values X , Y and Z , the x and y colour coordinates can be derived, and these coordinates determine the location of the light source $P(\lambda)$ in the chromaticity diagram.

$$x = \frac{X}{X+Y+Z} \quad (4)$$

$$y = \frac{Y}{X+Y+Z} \quad (5)$$

Pure colours are located along the contour of the chromaticity diagram, in the centre of which the white light area is situated.

As a standard for white light, the spectrum of black-body radiation (black-body radiator; BBR) is used. BBR

radiation is located in the chromaticity diagram (x , y) and its location is called the Planckian locus [19]. With the increasing temperature of the black body, the Planckian locus moves from the red wavelength area to the white central portion of the chromaticity diagram, as shown in Fig. 2.

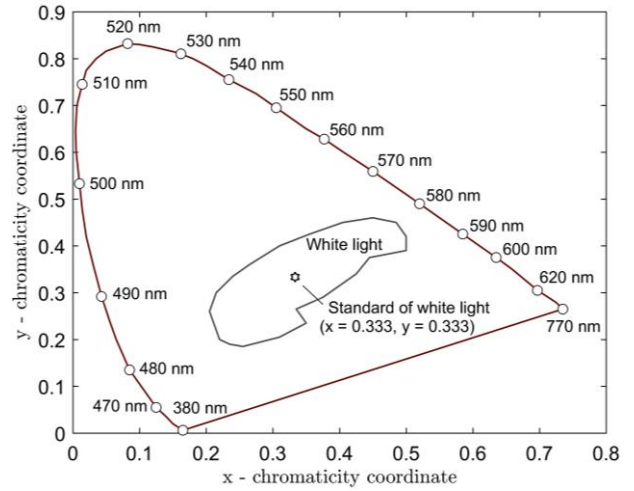


Fig. 2. The temperature of a Planck's black-body radiator

2.2. Colour rendering index (CRI)

Another important feature of the white light source is its ability to show true (i.e. rendered) colours of physical objects, such as plants, fruit or toys that are illuminated by it. The ability to render colours of an object is measured by the colour rendering index (CRI).

The colour rendering capability of the light source tested (the source tested) is evaluated by comparison with the colour rendering capability of the reference light source (the reference source).

For the specific determination of the CRI value of the source tested, the so-called test samples, which are actual physical objects, e.g. fruit, flowers, wood, furniture and clothing, are used. For the purpose of international standardization, a specific set of 14 colour samples tested was agreed upon, wherein the first eight of them are used to determine the CRI.

According to the CIE standard, the total average CRI is calculated as follows:

$$CRI = \frac{1}{8} \sum_{i=1}^8 CRI_i. \quad (6)$$

The values of CRI_i are calculated as follows:

$$CRI_i = 100 - 4.6\Delta E_i^*, \quad (7)$$

where ΔE_i^* represents the quantitative change in colour that occurs when the i th test colour sample is first illuminated by the reference source and then by the source tested. The calculation of individual CRI_i is set in such a way that, if there are no differences in colour rendering,

the sum of all its contributions was 100. Specific experimental determination of individual values ΔE_i^* is not quite trivial, but modern instruments have such algorithms built-in that they can easily determine the total CRI size of the source tested [20-21].

3. Experimental part

3.1. Sample preparation

In our experiments, we used a phosphor with cerium-doped yttrium aluminium oxide garnet particles ($Y_3Al_5O_{12}$: Ce or YAG: Ce; Phosphor Technology Ltd). The trademark of this phosphor is QMK58/F-U2, and, in this article, we further use the abbreviation U2 for this phosphor. We prepared 80 samples of U2 phosphor and PDMS. The first 40 samples had a weight ratio of 1:2 (U2:PDMS) and the other 40 samples had a weight ratio of 2:3 (U2:PDMS). Hereafter, these weight ratios of U2 phosphor in PDMS will be indicated as the weight ratio of 1:2 and the weight ratio of 2:3. First, according to the instructions in the datasheet, a pure PDMS mixture was

prepared, and this mixture was divided into two equal volume parts into each of which U2 phosphor was added according to the desired weight ratio. The mixture of these two weight ratios was then blended in a laboratory shaker for 180 minutes to ensure maximum homogenization of the mixture, and, subsequently, it was applied to microscope slides by spincoating at 500 rpm (revolutions per minute). For total curing, these samples were placed in an electric furnace where they were cured at 90°C for 45 minutes. The thickness of the layers thus produced was measured by two-plane focusing using the LPT 3113i-T microscope and was determined at $118 \pm 2 \mu\text{m}$ and $124 \pm 2 \mu\text{m}$ for the weight ratios 1:2 and 2:3 respectively.

3.2. Experimental setup

The experimental setup consisted of 150 W Lamp Housing LSH102, Halogen Lamp Power Supply (type LSN111), a Grating Monochromator (type Omni- λ 150), a sample holder, optical fibre (type M28L01-IC 400 μm 0.39NA), a spectrophotometer (type Ocean Optics), and a computer with the required software (please see Fig. 3).

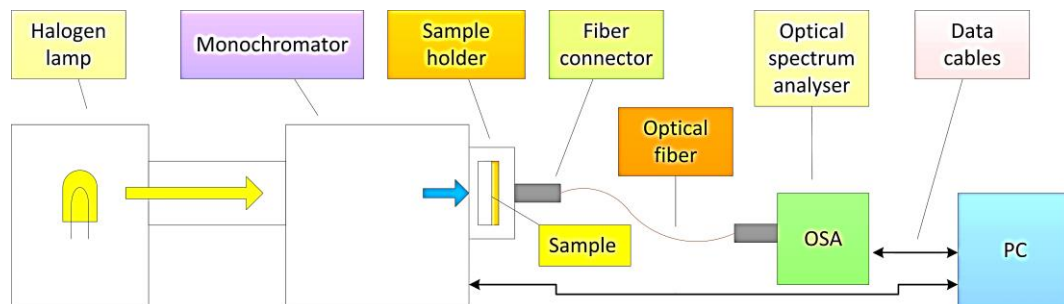


Fig. 3. Scheme of the experimental setup for the spectral measurement

3.3. CCT and CRI measurement

Measurement of CCT and CRI values was repeatedly performed. The samples were gradually inserted into a specially prepared sample holder and individual measurements were performed. The characteristics of the light generated by the luminescent layer of the samples for an excitation wavelength in the range from 440 nm to 470 nm with a 2 nm measurement step were examined. During this process, 30 CCT and CRI values for each of these measurement steps were automatically recorded in the time span of about 60 seconds. The resulting graphs of these measurements are shown in Figs. 4 to 6. For the sake of clarity, only the average values of all these measurements for both of U2:PDMS weight ratios are recorded in the graphs. The interconnection of the variable excitation wavelength and the corresponding changes in CCT and CRI can be seen in the graphs.

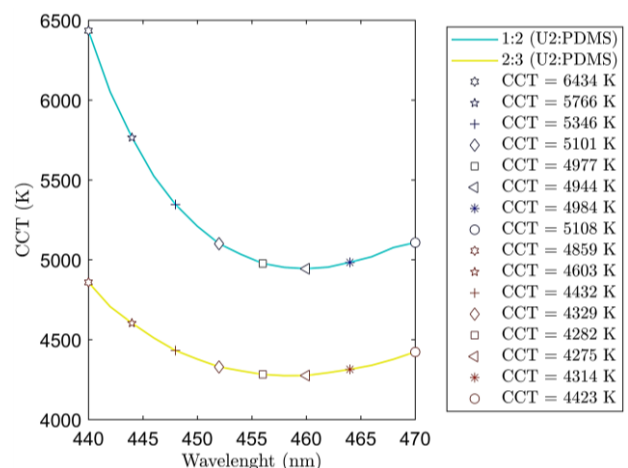


Fig. 4. The graph of CCT dependence on the excitation wavelength

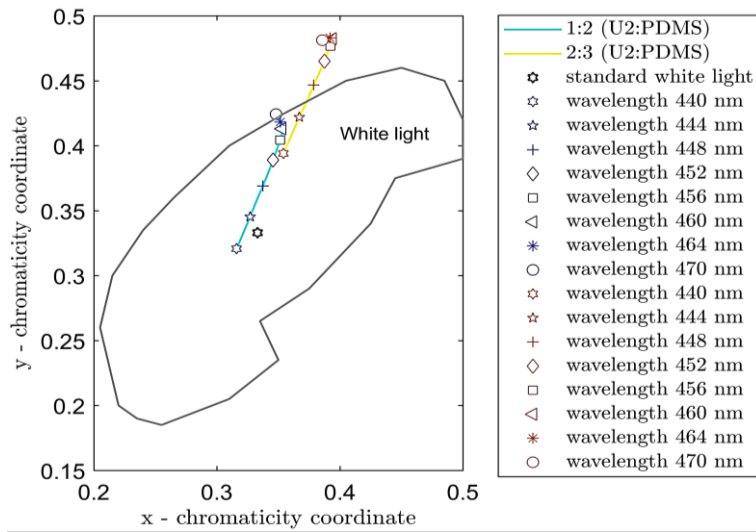


Fig. 5. The graph of dependence of changes in colour coordinates in relation to changes in the excitation wavelength

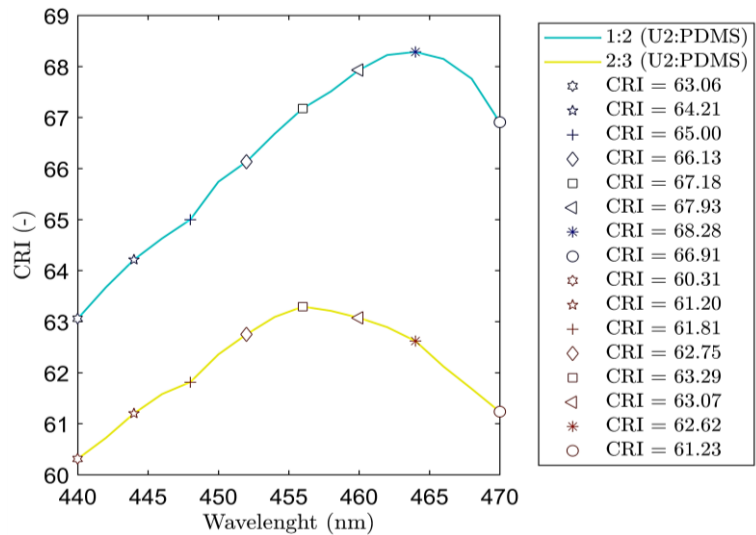


Fig. 6. The graph of CRI dependence on the excitation wavelength

Significant values in Graphs 4 to 6 are listed in Tables 1 and 2.

Table 2. The values of the CRI, CCT and the chromaticity coordinates for the selected excitation wavelengths. Weight ratio 2:3 (U2:PDMS)

Table 1. The values of the CRI, CCT and the chromaticity coordinates for the selected excitation wavelengths. Weight ratio 1:2 (U2:PDMS)

Wavelength (nm)	ratio 1:2 (U2:PDMS)			
	CRI (-)	CCT (K)	x (-)	y (-)
440	63.06	6438	0.315	0.321
444	64.21	5781	0.326	0.345
448	65.00	5332	0.337	0.369
452	66.13	5093	0.345	0.389
456	67.18	4975	0.350	0.404
460	67.93	4941	0.352	0.413
464	68.28	4979	0.351	0.418
470	66.91	5099	0.347	0.424

Wavelength (nm)	ratio 2:3 (U2:PDMS)			
	CRI (-)	CCT (K)	x (-)	y (-)
440	60.31	4861	0.353	0.394
444	61.20	4603	0.366	0.422
448	61.81	4418	0.378	0.447
452	62.75	4322	0.386	0.465
456	63.29	4282	0.390	0.475
460	63.07	4275	0.392	0.483
464	62.62	4316	0.390	0.484
470	61.23	4418	0.384	0.481

4. Discussion

The graphs in Figs. 4 to 6 show that the measured values of CRI, CCT and chromaticity coordinates x , y strongly depend on the excitation wavelength used and the weight ratio of U2 phosphor in PDMS. This dependence of the resulting measured values on the excitation wavelength appears to be related to the fact that also the conversion efficiency of U2 phosphor is dependent on the excitation wavelength. It follows that also the resulting ratio between the narrow blue excitation area and the broadband converted light strongly depends on the excitation wavelength used.

U2 phosphor achieves maximum conversion efficiency for an excitation wavelength of approximately 460 nm, which can be easily distinguished from the graph of CCT dependence on the excitation wavelength (see Figure 4). At the excitation wavelength of 460 nm, light with the lowest CCT value is generated. It is known that the lower the CCT value, the greater the share of broadband red and green spectral regions is. A higher CCT value, on the contrary, indicates a greater proportion of the blue spectral component of light. And since the excitation wavelength of 460 nm leads to the largest decrease in the CCT value, the smallest proportion of the blue spectral component of light must be present at this wavelength. This minimum blue spectral light component is caused by the maximum conversion efficiency of the phosphor for a given wavelength, which induces conversion of the major part of the blue component to a broadband component. The graph in Figure 4 also indicates that the CCT value greatly depends on the weight ratio of U2 in PDMS. The resulting CCT value for the lower weight ratio (1:2) is always bigger than for the higher weight ratio (2:3). At the weight ratio of 1:2, the blue excitation light reacts with a smaller amount of the phosphor than in the case of the weight ratio of 2:3 (U2:PDMS). It follows that for the weight ratio of 1:2 (U2:PDMS) a smaller portion of the blue excitation light is converted by the phosphor than in the case of the weight ratio of 2:3 (U2:PDMS). Therefore, at the weight ratio of 1:2 (U2:PDMS), a higher proportion of the blue spectral component remains in the light generated, so the resulting CCT value is always greater than in the case of the weight ratio of 2:3 (U2:PDMS).

The graph in Fig. 5 shows that the excitation wavelength and the weight ratio of U2 phosphor in PDMS also strongly affect the chromaticity coordinates values x , y in the chromaticity diagram. For the weight ratio of 1:2 and at an excitation wavelength in the range from 440 nm to almost 470 nm, the luminescent layer generates light falling within the white light area. Moreover, for excitation wavelengths in the range from 440 to 444 nm, it approximates to the standard white light emitter with the chromaticity coordinates $x = 0.333$ and $y = 0.333$. For the weight ratio of 2:3, the situation is different. The light generated by the luminescent layer with this weight ratio of phosphor U2 in PDMS is located in the white light region only for excitation wavelengths in the range from 440 to 446 nm. In addition, for this weight ratio of U2:PDMS, it is more distant from the white light standard.

The graph in Fig. 6 shows the dependence of CRI on the excitation wavelength for the weight ratios of 1:2 and 2:3. For the weight ratio of 1:2, the light generated by this luminescent layer has higher CRI values than for the weight ratio of 2:3. At the weight ratio of 1:2 and for the excitation wavelength of 464 nm, it achieves its maximum value $CRI = 68.28$. For the weight ratio of 2:3, it achieves its maximum value $CRI = 63.29$ at the excitation wavelength of 456 nm. In both cases, the maximum CRI value is reached in the relatively near vicinity of the excitation wavelength of 460 nm for which U2 phosphor has the maximum conversion efficiency. Nevertheless, CRI does not reach its maximum directly for this excitation wavelength of 460 nm. This is related to the fact that, for the high CRI value, the blue, green and red spectral components of the light generated must be in a certain balanced ratio. When using an excitation wavelength for which the phosphor has the maximum conversion efficiency, the blue spectral component will be significantly suppressed, and thus the appropriate ratio of the individual spectral components will be impaired.

5. Conclusion

We have revealed that the CCT, CRI values and the location in the chromaticity graph are strongly related to the excitation wavelength used and the weight ratio of U2 phosphor in PDMS for a specific luminescent layer thickness. When increasing the excitation wavelength from 440 nm to 460 nm, the CCT value decreased and reached its minimum for the excitation wavelength of 460 nm. This dependence applied similarly for both weight ratios of U2 phosphor in PDMS used and is related to the fact that, for the excitation wavelength of 460 nm, U2 phosphor achieves its maximum conversion efficiency. In terms of quality of white light, the weight ratio of 1:2, in which it was possible to tune the CCT values in the range of 6.438 K to 4.941 K using a variable excitation wavelength ranging from 440 to 460 nm, proved to be more appropriate. For this weight ratio of U2 in PDMS and for excitation wavelengths in the range from 440 to 444 nm, the generated light approximated, to the greatest possible extent, to standard white light with respect to the location in the chromaticity diagram. In terms of the CRI value, the weight ratio of 1:2 was also more appropriate when the maximum value $CRI = 68.28$ was reached at the excitation wavelength of 464 nm. The thickness of the luminescent layer used for the weight ratio of 1:2 was $118 \pm 2 \mu\text{m}$.

This research shows that by changing the excitation wavelength and weight ratio of phosphor in the luminescent layer, it is possible to vary the CCT, CRI values and the location in the chromaticity diagram in a significant range. This change will probably also be strongly related to the thickness of the luminescent layer used, but the direct examination of the dependence of the CCT, CRI parameters and the chromaticity coordinates x , y on the thickness of the luminescent layer was not the content of this article. From the results of this research

presented, it can be concluded that a suitable combination of the excitation wavelength and the parameters of the luminescent layer can be achieved by optimizing the desired values of CCT, CRI and the location in the chromaticity diagram.

Acknowledgments

This article was supported by the Ministry of Education of the Czech Republic (Projects No. SP2019/80, SP2019/85). This work was supported by the European Regional Development Fund in Research Platform focused on Industry 4.0 and Robotics in Ostrava project, CZ.02.1.01/0.0/0.0/17_049/0008425 within the Operational Programme Research, Development and Education.

References

- [1] G. Feng, W. Jiang, J. Liu, C. Li, Q. Zhang, L. Miao, Q. Wu, *Ceramics International* **44**(7), 8435 (2018).
- [2] L.-C. Chen, Z.-L. Tseng, W.-W. Chang, Y. W. Lin, *Ceramics International* **44**(4), 3868 (2018).
- [3] H. Zhou, J. Zou, B. Yang, W. Wu, M. Shi, Z. Wang, Y. Liu, M. Li, G. Zhao, *Journal of Non-Crystalline Solids* **481**(1), 537 (2018).
- [4] T. Tang, S. Zhou, X. Yi, S. Zhang, D. Hao, X. Shao, *Journal of the American Ceramic Society* **100**(6), 2590 (2017).
- [5] J. Wang, S. W. R. Lee, H. Zou, H., *Proceedings of the 2016 IEEE 18th Electronics Packaging Technology Conference*, (2016).
- [6] G. Gu, W. Xiang, C. Yang, W. Fan, Y. Lv, Z. Zhang, X. Liang, *Science of Advanced Materials* **8**(7), 1354 (2016).
- [7] M. Gong, X. Liang, Y. Wang, H. Xu, L. Zhang, W. Xiang, *Journal of Alloys and Compounds* **664**, 125 (2016).
- [8] Y. Du, C. Shao, Y. Dong, Q. Yang, *Journal of Display Technology* **12**(4), 323 (2016).
- [9] M. Gong, W. Xiang, J. Huang, C. Yin, X. Liang, *RSC Advances* **5**(92), 75781 (2015).
- [10] J. Huang, X. Liang, W. Xiang, M. Gong, G. Gu, J. Zhong, D. Chen, *Materials Letters* **15**, 31 (2015).
- [11] H.-Y. Lin, Z.-Y. Tu, P.-C. Ku, C.-C. Lin, H.-C. Kuo, *Proc. of SPIE* **9383**, (2015).
- [12] L.-C. Chen, W.-W. Lin, J.-W. Chen, *Advances in Materials Science and Engineering* **2015**, (2015).
- [13] T. Güner, D. Köseoğlu, M. M. Demir, *Optical Materials* **60**, 422 (2016).
- [14] T. Güner, U. Şentürk, M. M. Demir, *Optical Materials* **72**, 769 (2017).
- [15] J. Jia, H.-S. Jia, A.-Q. Zhang, Q.-Q. Shen, D.-X. Li, X.-G. Liu, *Chinese Journal of Luminescence* **38**(11), 1493 (2017).
- [16] J. Jargus, J. Nedoma, M. Fajkus, M. Novak, V. Vasinek, V., *Proc. of SPIE* **10209**, (2017).
- [17] J. Jargus, J. Nedoma, M. Fajkus, M. Novak, L. Bednarek, V. Vasinek, *Proc. of SPIE* **10232**, (2017).
- [18] *CIE Commission Internationale de l'Eclairage Proceedings*, Cambridge University Press, Cambridge, 1931.
- [19] E. F. Schubert, *Light-emitting diodes*, Cambridge University Press, New York, second edition, 2006.
- [20] *CIE Commission Internationale de l'Eclairage Proceedings*, Cambridge University Press, Cambridge, 1995.
- [21] M. Bass, E. W. Stryland, A. R. Williams, W. Wolfe, *Handbook of optics*, Library of Congress, 1995.

*Corresponding author: jan.nedoma@vsb.cz